universität wien

Microphysics-Parametrizations in WRF

Lukas Kugler

Report for the course FUNDAMENTALS OF ATMOSPHERIC MODELLING
at the Department of Meteorology and Geophysics, University of Vienna
Submitted: 2017-06-21; Last Update: 2017-07-03

This study explores microphysics parametrizations available in the Weather Research and Forecasting Model and its effects on precipitation and (thermo-)dynamics based on theoretical analysis and a case study simulating a cyclogenesis event in the Mediterranean Sea. The precipitation field transitions from rain to snow in the eastern part of Austria with shallow cold air advection from northerly directions. The analysis quantifies the difference between two model runs using different microphysics schemes. For this, the resemblance between the runs is analyzed using summed difference, 1-norm and ∞-norm of timeseries of precipitation and shows the different evolutions of outgoing long-wave radiation on a map.

1 Basics

1.1 Resolving Cloud Physics

As the explicit simulation of each individual droplet/hydrometeor in a cloud is an overwhelming task, cloud dynamics are parameterized. This happens either explicitly in a so called cloud-resolving model on scales below 1 km so that clouds and their associated processes can be represented directly on the model grid (Stensrud, 2009). In contrast convective parametrization only simulate the cumulative effects of clouds implicitly. Though it is believed that explicit representation is superior, both methods are used today, complementing each other and, as was shown 1988, do not lead to double counting the heating or moistening produced by convection (Stensrud, 2009). Another interesting effect was also observed: Not only reducing the grid spacing from 2 km to 500 m can alter the behavior of mesoscale phenomena, but also reducing it from 1 km to 125 m.

1.2 Cloud-Microphysics

In addition to the well-known fundamental equations of hydrodynamics a few other equations have to be modelled to produce cloud water and rain. These processes also have an impact to dynamics through the temperature change associated with phase changes of water. This feedback process is quite large as the energy associated with condensing one gram of water is capable of increasing the temperature of one kilogram of air by almost nine Kelvin.

A basic law in cloud-physics is the following equation which describes the change of enthalpy of moist air. Additionally to the temperature effect of dry enthalpy, phase changes of water may occur:

$$\mathrm{d}h(T, q_v, q_l) = c_p \,\mathrm{d}T + h_v \,\mathrm{d}q_v + h_l \,\mathrm{d}q_l + h_i \,\mathrm{d}q_i \tag{1}$$

where c_p refers to the specific heat at constant pressure, h_v, h_l and h_i refer to the specific enthalpy of vapor, liquid water and ice. The adjacent differentials refer to the change of mixing ratios for vapor, liquid and ice. Neglecting rain, one would have conservation among the three phases: $\mathrm{d}q_v + \mathrm{d}q_l + \mathrm{d}q_i = 0$.

The temperature effect due to condensation or evaporation (Stensrud, 2009) is given by

$$\mathrm{d}\theta = \frac{L_v}{c_p} \left(\frac{p_0}{p}\right)^{\frac{R}{c_p}} \mathrm{d}q_l \tag{2}$$

where L_v and R refer to the latent heat of vaporization and the individual gas constant. $\mathrm{d}q_l$ is the mass of condensed or evaporated water.

As diffusion is the most important driver for droplet growth at early stages (Wallace and Hobbs, 2006), one has to model the vapor pressure around a droplet because it determines the diffusion rate to/from the droplet and thus the growth rate of a droplet. The well-known Köhler curve describes the relation between saturation ratio and a critical droplet radius above which a droplet may grow and below which it will decline.

An important categorization shall not be ommitted: If one wants to describe clouds warmer than -10 °C, then one does typically does not need to account for the ice phase as ice crystals typically are observed starting at temperatures of -15 °C (Stensrud, 2009). From -15 °C to -40 °C both liquid and frozen hydrometeors are to be expected. At temperatures of -40 °C and below water droplets freeze homogeniously, even in completely aerosol/cloud-condensation-nuclei free air. Those threshold-temperatures are not strict barriers but the probability of, e.g., finding a liquid droplet at T <-40°C goes to zero very rapidly.

Further aspects like collision and coalescence, freezing, graupel processes, the Bergeron-Wegener-Findeisen

process or else will not be discussed.

1.3 Saturation adjustment vs. prediction

The question how much vapor is condensed is still open at this point. In common microphysics parametrizations, the condensation rate C is calculated at the end of an integration step such that the vapor pressure e (over a flat surface) is equal to the saturation vapor pressure e_s. This procedure is called saturation adjustment as it condenses exactly that much vapor so that the relative humidity is again at 100 %, i.e. saturation. To calculate that amount, one assumes that the adjustment process takes place at constant surrounding pressure, uses the Clausius-Clapeyron equation

$$\frac{\mathrm{d}e_s}{\mathrm{d}T} = \frac{L_v e_s}{R_v T^2} \tag{3}$$

and an approximation for the mixing ratio $e = q_v p/\varepsilon$ to describe how much vapor has to be removed from the parcel to remain at 100 % saturation, given a reduction in temperature after lifting the parcel:

$$\underbrace{\mathrm{d}q_{vs}}_{\text{decrease in vapor mass}} = \frac{L_v q_{vs}}{R_v T^2} \underbrace{\mathrm{d}T}_{\text{decrease in temperature}} \tag{4}$$

This equation states how much the mixing ratio has to be decreased, i.e. how much vapor has to be condensed, for a given decrease in temperature (after lifting an air parcel for some height) so that the resulting vapor pressure is equal to the saturation vapor pressure.

Saturation prediction In contrast to this simplification, an explicit prediction of vapor pressure[1] is used in very few microphysics parametrizations. It leads to less condensed vapor because the vapor pressure is not adjusted to saturation vapor pressure in each timestep, but may be well over 100 % RH. As growing droplets in general need supersaturation[2] to achieve saturation with respect to their spherical shape and thereby growth in mass, the mixing ratio of vapor is increased at the cost of a lower ratio for liquid.

Stensrud (2009) surveys that all single-moment bulk microphysical schemes and most double-moment bulk schemes use bulk condensation, i.e. saturation adjustment instead of saturation prediction.

[1] the term in literature is *saturation prediction*
[2] with respect to a flat surface of water

1.4 Bulk vs. bin microphysical representation

Microphysical parametrizations may be grouped into 'bulk' and 'bin' approaches. Bulk methods use a specified functional form for the particle size distributions and predict the mixing ratio of the liquid and, sometimes, total particle concentration. Schemes that predict only the mixing ratio are called single-moment schemes, while the ones that predict both variables are called double-moment schemes (Stensrud, 2009). Bin schemes maintain dozens of variables to represent the particle distribution by a high number of categories.

One common and important assumption in many schemes is that cloud water and the smallest cloud ice particles do not move relative to the flow, so they are simply advected with the flow, both horizontally and vertically. Precipitating particles (raindrops, snow, graupel, and hail), on the other hand, have significant fall speeds and move relative to the flow (Stensrud, 2009).

2 Parametrizations in WRF

As the number of available parametrizations in WRF (17 for Version 3.8) is much too high to describe each one in this report, only two of them are picked: The WRF Single-Moment 3-class scheme (called 'WSM3', option 3) and the Thompson et al. scheme (option 8).

2.1 WSM3

The WRF Single-Moment 3-class scheme is described in the WRF-User's Guide (V3.8) as "a simple, efficient scheme with ice and snow processes suitable for mesoscale grid sizes". It is published in Hong et al. (2004) and models three categories of hydrometers: vapor, cloud water/ice, and rain/snow, which is a so-called simple-ice scheme. It follows Dudhia (1989) in assuming cloud water and rain for temperatures above freezing, and cloud ice and snow for temperatures below freezing. This scheme is computationally efficient for the inclusion of ice processes, but lacks supercooled water and gradual melting rates (Skamarock, 2008).

It models ice phase processes, but does not account for mixed phase processes (WRF User-Guide).

As single moment scheme it only predicts the mixing ratios, but assumes a particle distribution rather than predicting it. It includes ice sedimentation and other ice-phase parametrizations. A major difference from other approaches is that a diagnostic relation is used for ice number concentration that is based on ice mass content rather than temperature. As with WSM5 and WSM6, the freezing/melting processes

are computed during the fall-term sub-steps to increase accuracy in the vertical heating profile of these processes. The order of the processes is also optimized to decrease the sensitivity of the scheme to the time step of the model (Skamarock, 2008).

2.2 Thompson

The 'new' Thompson et al. scheme models ice, snow and graupel processes suitable for high-resolution simulations. It adds rain number concentration and is an update from the one in WRF Version 3.0. The main publication is Thompson et al. (2004) but build upon a parametrization by Reisner et al. (1998) which was already included in the MM5 mesoscale model.

It incorporates a large number of improvements with regard to older versions and employs many techniques found in far more sophisticated spectral/bin schemes using look-up tables. Unlike any other bulk parametrization, the assumed snow size distribution depends on both ice water content and temperature and is represented as a sum of exponential and gamma distributions. Furthermore, snow assumes a non-spherical shape with a bulk density that varies inversely with diameter as found in observations and in contrast to nearly all other BMPs that assume spherical snow with constant density (Skamarock, 2008).

New features specific to this version of the bulk scheme compared older versions include (Skamarock, 2008)

- generalized gamma distribution shape for each hydrometeor species,
- non-spherical, variable density snow, and size distribution matching observations,
- y-intercept of rain depends on rain mixing ratio and whether apparent source is melted ice,
- y-intercept of graupel depends on graupel mixing ratio,
- a more accurate saturation adjustment scheme,
- variable gamma distribution shape parameter for cloud water droplets based on observations,
- look-up table for freezing of water drops,
- look-up table for transferring cloud ice into snow category,
- improved vapor deposition/sublimation and evaporation,
- variable collection efficiency for rain, snow, and graupel collecting cloud droplets,
- improved rain collecting snow and graupel.

3 Case study: 2016-11-12 12 UTC + 36 h

3.1 Synoptic situation

The large scale flow over europe is dominated by a trough over europe which is already in the process of being cut off by an intense low over iceland with mean sea level pressure below 975 hPa which advects subtropical air with equivalent potential temperatures θ_e above 45 °C. In contrast can polar air with θ_e around 5 °C be observed from northern germany through poland until just north of ukraine. The system of interest developed in the course of the previous day as the upper air trough moved into the Ligurian Sea and the circulation initiated with cold air pushing through the Rhone Valley into the Mediterranean Sea where GFS simulated gusts of about 45 knots the mentioned day. As the surface low travels eastward from the Ligurian Sea, positive temperature advection combined with positive vorticity advection result in widespread precipitation, locally enhanced by orography. Attention shall be drawn to shallow advection of extremely cold air ($\theta \approx 0$) from Poland southward through the so called Moravian Gate[3] (about 310 m MSL) which is one of very few gaps through the Carpathian Mountains in the east and the Sudetes (max. 1600 m MSL) in the west.

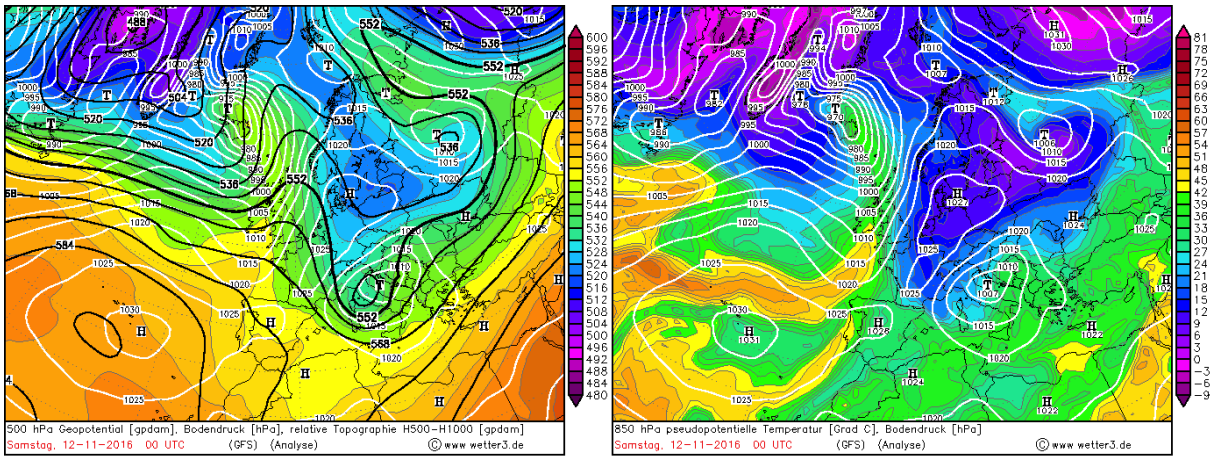

Figure 1: Synoptic situation; left: geopotential distribution at 500 hPa (black contours), relative topography 500-1000 hPa (color coded); right: surface pressure (white contours), distribution of equivalent potential temperature at 850 hPa (color coded); source: *wetter3.de*

[3] German: 'Mährische Pforte'

PARAMETER	SETTING	PARAMETER	SETTING	PARAMETER	SETTING
mp_physics	**3 / 8**	cudt	5	diff_6th_opt	0
ra_lw_physics	1	isfflx	1	diff_6th_factor	0.12
ra_sw_physics	1	ifsnow	1	base_temp	290
radt	12	icloud	1	damp_opt	0
sf_sfclay_physics	1	surface_input_source	3	zdamp	5000
sf_surface_physics	2	num_soil_layers	4	dampcoef	0.2
bl_pbl_physics	1	w_damping	0	khdif	0
bldt	0	diff_opt	1	kvdif	0
cu_physics	1	km_opt	4	non_hydrostatic	.true.
sf_urban_physics	0	moist_adv_opt	1	-	-
num_land_cat	20	scalar_adv_opt	1	-	-

Table 1: Physics and dynamics settings made to `namelist.input`

3.2 WRF-Setup

The setup consists of two domains: one 'mother' domain at 12 km grid resolution and one nested domain at 4 km grid resolution. The time step is fixed at 72 seconds / 24 seconds. The outer domain consists of 120 $\times$ 120 grid points while the inner domain is 250 $\times$ 211 grid points. The vertical dimension is covered by 38 levels. Dynamics feedback to the outer domain is turned on. The geographical setting may be seen from figure 2. Notice that the highest mountain is about 2900 m in the 12 km domain and about 3600 m in the 4 km domain. A special grid box (see figure 2) of 14 $\times$ 10 grid points (i.e. 56 $\times$ 40 km) was defined to sample atmospheric variables inside the inner domain.

All settings related to physics and dynamics are listed in table 1.

The initial and boundary values for the model run were provided through the *NCEP GFS 0.25° global forecast grids historical archive* by the National Centers for Environmental Prediction (2015).

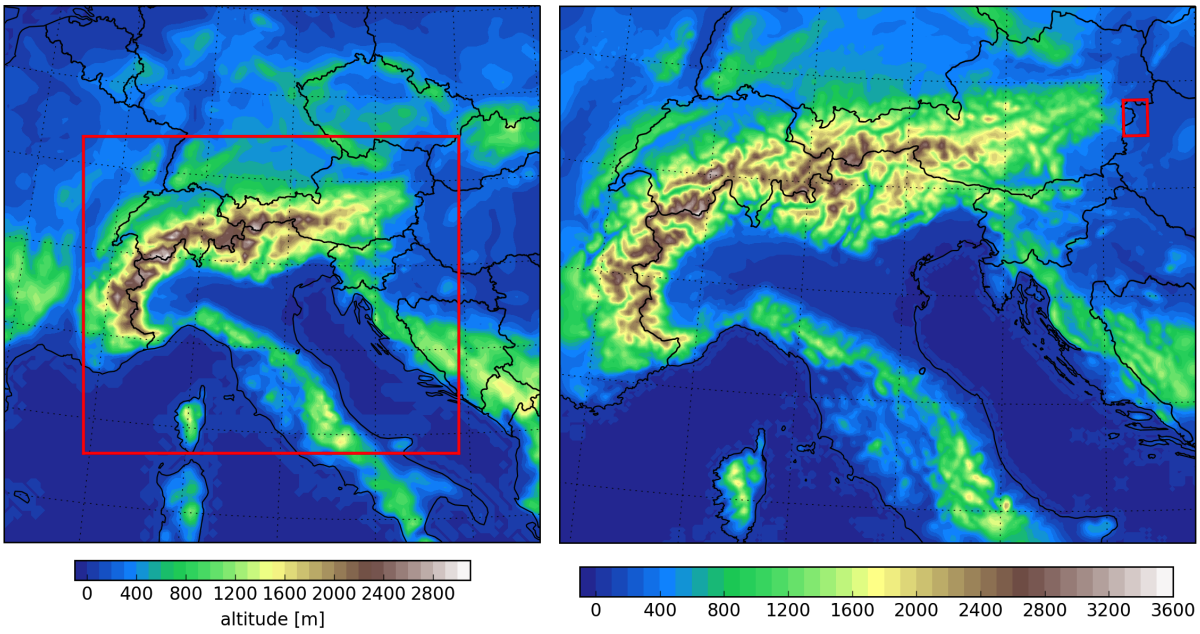

Figure 2: Left: Outer domain at Δx : 12 km (whole plot) with one nested domain (red box); Right: nested domain at Δx : 4 km with a sampling box (red square) for further investigations; color coded according to model topography

4 Results

A first insight into direct model output reveals quite realistic results in terms of potential temperatures and accumulated precipitation over 30 hours (see figure 3). While orographically exposed locations received more than 120 mm, a 30 mm is also observed in flat terrain.

To compare the results of two runs, one can step back and look at the top-of-atmosphere outgoing longwave radiation (OLR). Even 12 hours after the initiation of the model, one can see substantial differences in the cloud formations (figure 4). While the WSM3 only resulted in very limited total cloud cover, the Thompson scheme resulted in a exceptionally distinctive warm front shield of

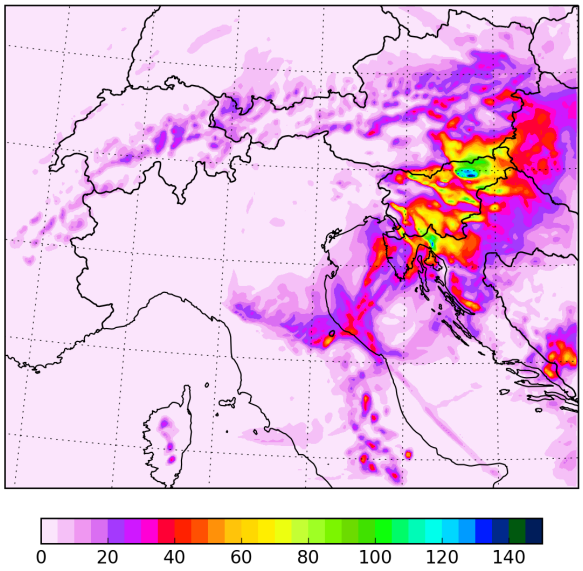

Figure 3: Thompson accumulated precipitation [mm] from 11-11 12z to 11-12 18z

cirrus clouds and a cold front which is cut off in a straight line by descending air behind it.

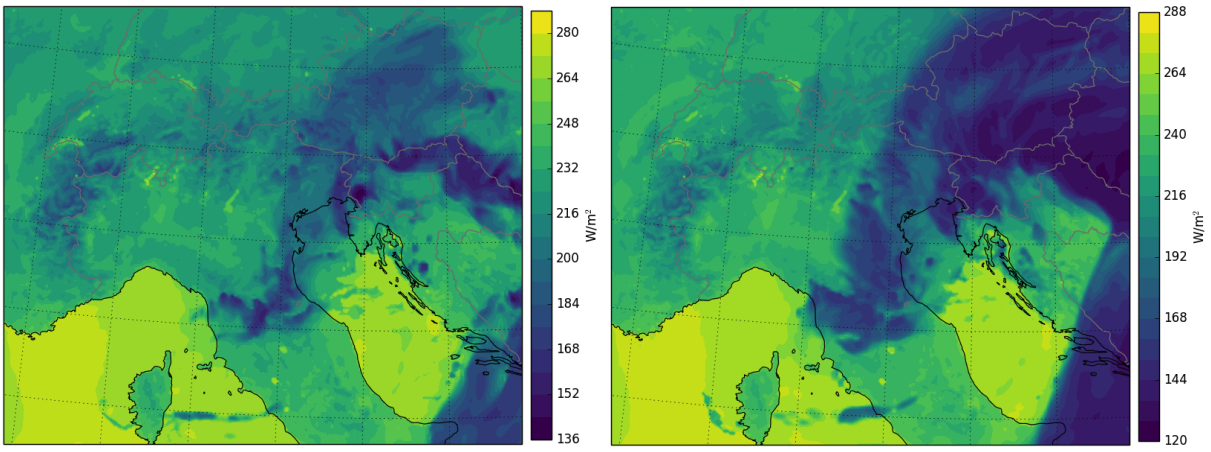

Figure 4: OLR 2016-11-12, 00 UTC; left: WSM3 scheme, right: Thompson scheme

Even four hours later (see figure 5) the difference is visible in that a back-bent occlusion type of cloud strikes the north-eastern part of austria again, whereas in the WSM3 run the radiation is less and therefore there is probably less cloud cover in total, or only low-level clouds.

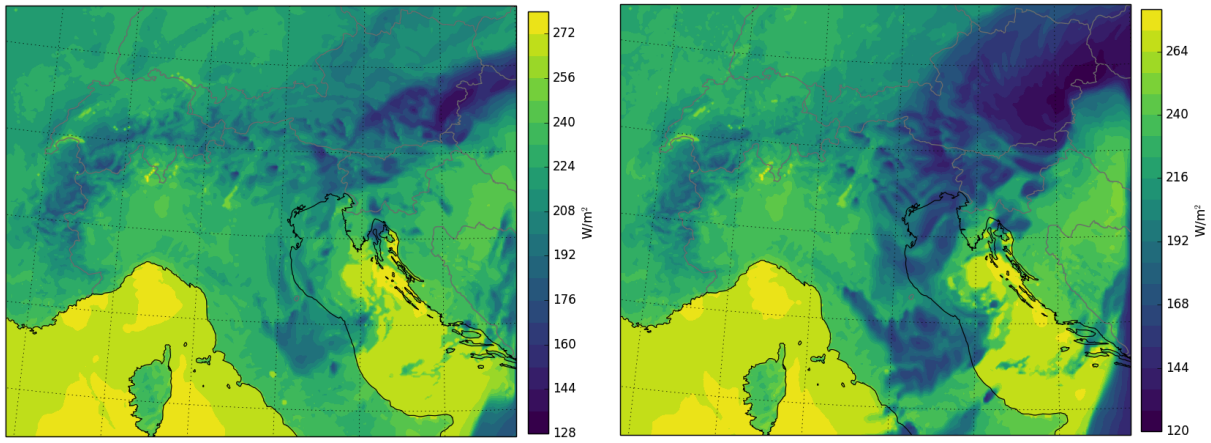

Figure 5: OLR 2016-11-12, 04 UTC; left: WSM3 scheme, right: Thompson scheme

To show the similarity of the precipitation field one may show (1) timeseries of a certain location or averaged over an area, (2) differences of the field in time or space and (3) correlations of the associated anomalies in time or space.

For (1) one may use one specific location, i.e. grid point. But that is the least representative for a whole domain. One may use an average over the whole domain, but that may lead to averaging-out of

interesting or characteristic phenomena. For that, the sampling box comes into use as averaging space.

Figure 6 shows the hourly precipitation of each run, averaged over the sampling box. What can be seen is quite a high similarity, but Thompson starts earlier and produces more precipitation than WSM3. Figure 7 shows the same data, but accumulates the precipitation (since model initialization).

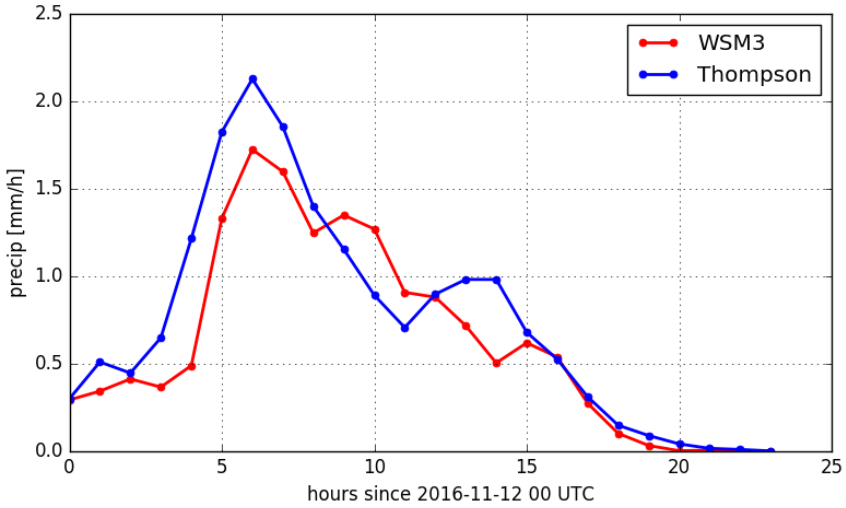

Figure 6: Hourly precipitation, average value within the sampling box

One may wonder how good the correlation over the whole domain is for each grid point. The answer is, that the correlation is above 90 % for quite the whole domain (not shown). For the previously shown OLR the numbers are quite different: Figure 8 shows that these correlation coefficients are below 50 % for most of the domain.

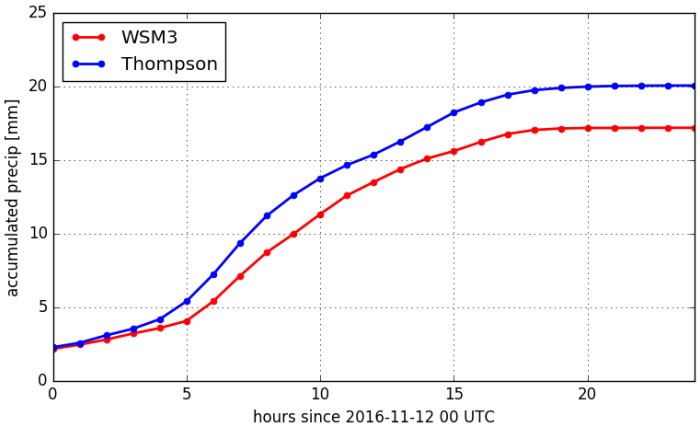

Figure 7: Accumulated precipitation since model initiation (previous day, 12 UTC), averaged over the sampling box

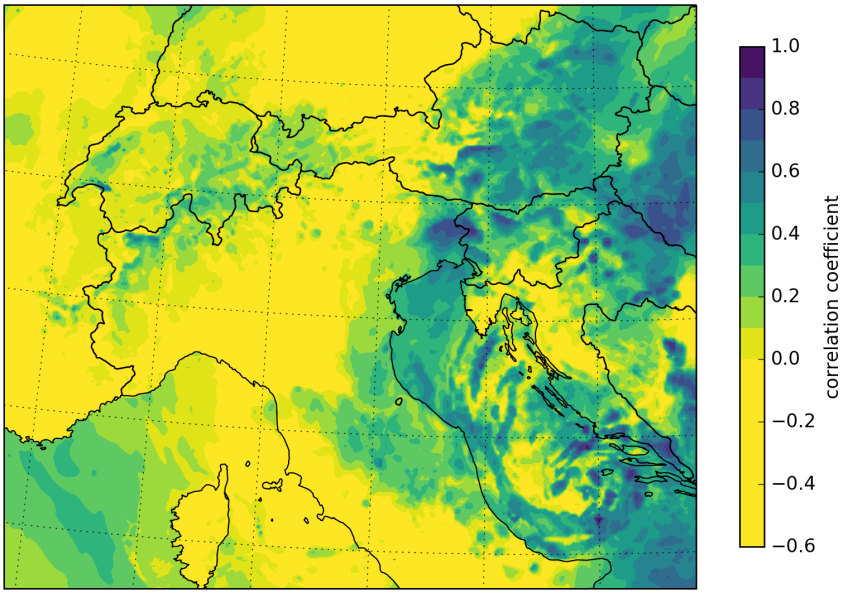

Figure 8: Correlation of the timeseries of TOA outgoing longwave radiation as a function of latitude and longitude

A simple, but appropriate measure to see whether one run simulated a pattern in precipitation where the other one did not, one can calculate the difference of accumulated precipitation of both runs at each gridpoint, as plotted in figure 9.

A downside to the ordinary difference is, that if there is a phase shift of precipitation, the values may compensate and show no difference at all. To avoid this, one can compute the absolute value of the difference, i.e. the 1-norm of a precipitation timeseries:

$$\sum_i |\text{precip\_1h}_{a,i} - \text{precip\_1h}_{b,i}| \tag{5}$$

It sums the absolute difference in hourly precipitation between the two runs and is shown in figure 10.

Lastly a measure to quantify the maximum difference at any hour in the timeseries: the ∞-norm,

$$\max_i |\text{precip\_1h}_{a,i} - \text{precip\_1h}_{b,i}| \tag{6}$$

describes the maximum difference in hourly intensity [mm/1h] over 24 hours and may be seen in figure 11.

In general, WSM3 led to slightly more precipitation on the whole domain[4] compared to Thompson.

[4] about 0.427 mm average over all gridpoints with precipitation > 0 mm; sum over whole domain: 19800 mm

In particular there were some convective events on the coastline of Croatia and one in the area of lake Balaton in Hungary where WSM3 produced precipitation, whereas Thompson did not. Considering stratiform precipitation, Thompson led to higher precipitation in most parts of Austria, where there was mostly solid precipitation.

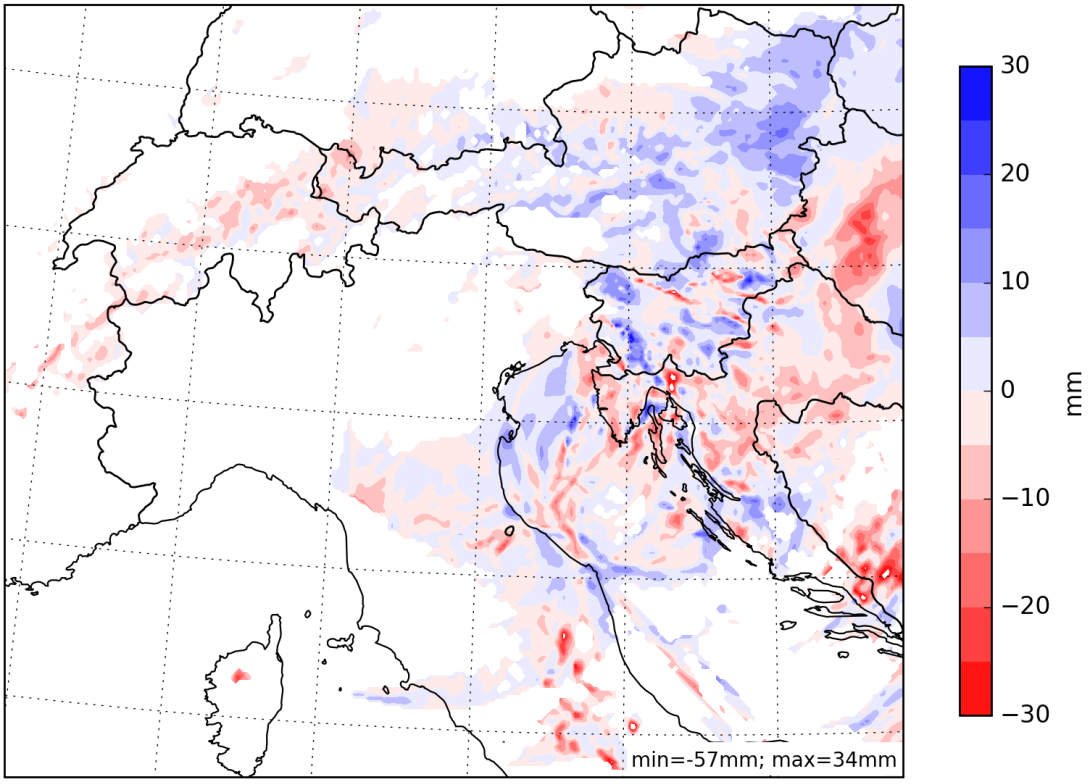

Figure 9: The difference "Thompson - WSM3" in accumulated precipitation over 36 hours before 2016-11-13 00 UTC

While the 1-norm shows the run differences to be large in flat areas of Hungary and areas with orographic forcing in coastal areas of Croatia and Bosnia (maybe convectively enhanced), the intensity difference (∞-norm) field is quite dotty. This is clear because one will expect high intensity only in convective systems which mostly limited to around 20 km in space.

The most interesting part is the area northwest of the sampling area, where one finds intensity differences above 6 mm/h which is quite high, given that there were no convective effects. The summed differences also show deviations of up to 20 mm in that area over 24 hours. Further investigation on this feature is needed, as the temperature in this area is below 0 °C (not shown) and the involved ice processes could expose how the different microphysics formulas affect snow intensity, etc.

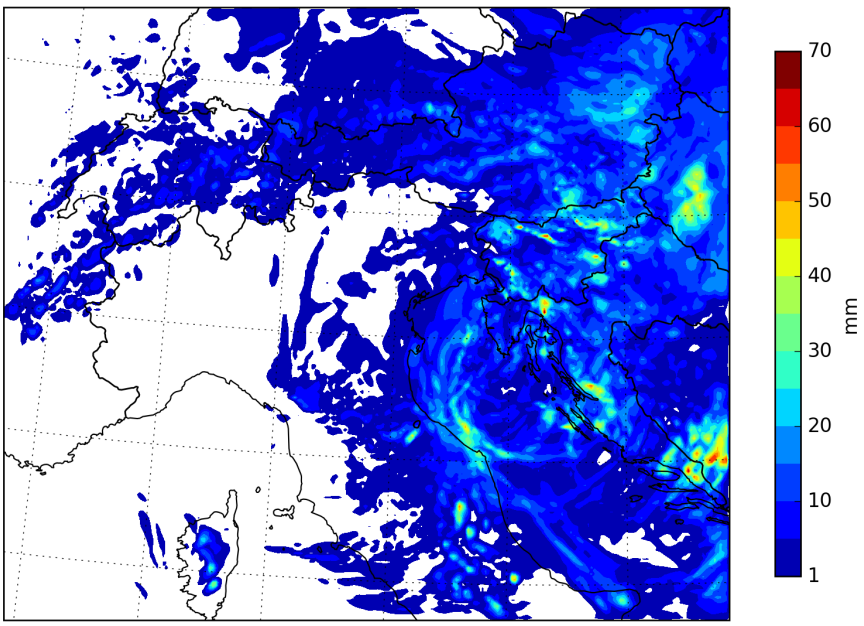

Figure 10: The 1-Norm of the timeseries of hourly precipitation over 36 hours, i.e. the sum over the absolute differences between the two runs.

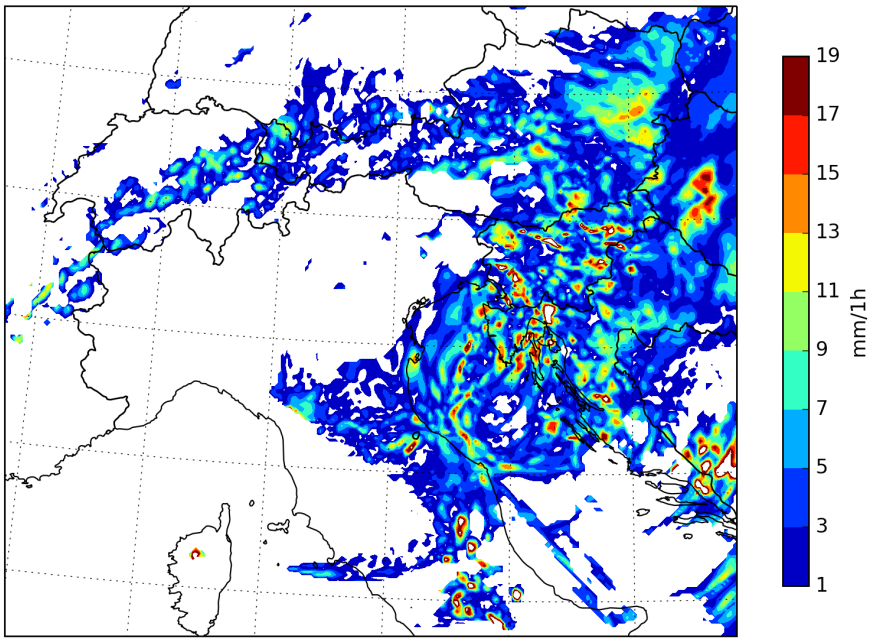

Figure 11: The ∞-Norm of the timeseries of hourly precipitation over 36 hours, i.e. the maximum deviation between the two runs. The maximum difference on the whole domain is 56 mm/1h.

The spot in southwestern Hungary is most probably associated with the occlusion point of the frontal system as can be seen in the OLR figures. Even though the frontal system was simulated more intense in the Thompson scheme in terms of a more realistic picture in OLR, the higher precipitation in Hungary was found with WSM3.

To conclude, one has to remind him/herself that the microphysics also has impact on the dynamics of the system and this report could scratch the surface, describing some effects of microphysics parametrizations. More interesting phenomena could still lie secretly hidden in the fields of cloud water and ice. Another study would be needed to investigate the found deviations north-east of the sampling box. The author suspects a correlation between the choice of the scheme and whether there was rain or snow in environments around 0 °C and in which intensity.

References

Hong, S.-Y., J. Dudhia, and S.-H. Chen, 2004: A revised approach to ice microphysical processes for the bulk parameterization of clouds and precipitation. *Monthly Weather Review*, **132 (1)**, 103–120.

National Centers for Environmental Prediction, N. U. D. o. C., National Weather Service, 2015: Ncep gfs 0.25 degree global forecast grids historical archive. Research Data Archive at the National Center for Atmospheric Research, Computational and Information Systems Laboratory, Boulder CO, URL https://doi.org/10.5065/D65D8PWK.

Pieri, A. B., J. von Hardenberg, A. Parodi, and A. Provenzale, 2015: Sensitivity of precipitation statistics to resolution, microphysics, and convective parameterization: A case study with the high-resolution wrf climate model over europe. *Journal of Hydrometeorology*, **16 (4)**, 1857–1872.

Reisner, J., R. M. RaSmuSSen, and R. Bruintjes, 1998: Explicit forecasting of supercooled liquid water in winter storms using the mm5 mesoscale model. *Quarterly Journal of the Royal Meteorological Society*, **124 (548)**, 1071–1107.

Skamarock, W., 2008: A description of the advanced research wrf version 3. Tech. rep., NCAR/TN-475+ STR.

Stensrud, D. J., 2009: *Parameterization schemes: keys to understanding numerical weather prediction models*. Cambridge University Press.

Thompson, G., R. M. Rasmussen, and K. Manning, 2004: Explicit forecasts of winter precipitation using an improved bulk microphysics scheme. part i: Description and sensitivity analysis. *Monthly Weather Review*, **132 (2)**, 519–542.

Wallace, J. M., and P. V. Hobbs, 2006: *Atmospheric science: an introductory survey*, Vol. 92. Academic press.